

---

---

OPTICAL  
PROPERTIES

---

---

## Infrared Absorption Spectra of a $\text{Nd}_{0.5}\text{Ho}_{0.5}\text{Fe}_3(\text{BO}_3)_4$ Crystal

Yu. V. Gerasimova, S. N. Sofronova, I. A. Gudim, A. S. Oreshonkov,  
A. N. Vtyurin, and A. A. Ivanenko

*Kirensky Institute of Physics, Siberian Branch, Russian Academy of Sciences,  
Akademgorodok 50, Krasnoyarsk, 660036 Russia*

*e-mail: jul@iph.krasn.ru, ssn@iph.krasn.ru*

Received April 27, 2015

**Abstract**—Infrared absorption spectra of a  $\text{Nd}_{0.5}\text{Ho}_{0.5}\text{Fe}_3(\text{BO}_3)_4$  crystal in the spectral range of 30–1700  $\text{cm}^{-1}$  have been measured at temperatures from 6 to 300 K. The experimental spectra have been analyzed based on the semiempirical calculation of the lattice dynamics and the analysis of correlation diagrams of borate complexes. No changes associated with structural phase transitions have been detected in the temperature range of measurements; the effect of magnetic ordering on the infrared absorption spectra has not been observed.

DOI: 10.1134/S106378341601011X

### 1. INTRODUCTION

Recent studies of rare-earth ferrobates with the general formula  $\text{ReFe}_3(\text{BO}_3)_4$  showed that the majority of compounds of this family belong to a multiferroic class [1–4]. The presence of two subsystems—iron and rear-earth ions—results in a diversity of properties. Despite the fact that the Fe–Fe exchange dominates over the indirect exchange of rare-earth elements, the orientation of the magnetic moments of iron ions with respect to crystallographic axes is determined by the type of the rare-earth ion. Either an easy-axis antiferromagnetic structure with the spins of iron ions ordered along the trigonal axis  $c$  ( $\text{Re} = \text{Dy}, \text{Tb}, \text{Pr}$ ) or an easy-plane structure ( $\text{Re} = \text{Nd}, \text{Eu}, \text{Er}$ ) with the spins of iron ions ordered in the  $ab$  plane perpendicular to the  $c$  axis of the crystal occur [5].

In addition, the structure of the compound is affected by the radius of the rear-earth ion: at high temperatures, all crystals of the  $\text{ReFe}_3(\text{BO}_3)_4$  family possess a trigonal structure, which belongs to space group  $R32$ . This structure remains unchanged down to ultimately low temperatures in the compounds with larger ionic radii ( $\text{Re} = \text{La}, \text{Ce}, \text{Pr}, \text{Nd}, \text{Sm}$ ), whereas a structural phase transition occurs in the compounds with a smaller ionic radii ( $\text{Re} = \text{Eu}, \text{Gd}, \text{Tb}, \text{Dy}, \text{Ho}, \text{Er}$ ).

The subject of our study was chosen to be a  $\text{Nd}_{0.5}\text{Ho}_{0.5}\text{Fe}_3(\text{BO}_3)_4$  solid solution. It is of interest because the properties of parent compounds— $\text{NdFe}_3(\text{BO}_3)_4$  and  $\text{HoFe}_3(\text{BO}_3)_4$ —differ quite significantly:  $\text{HoFe}_3(\text{BO}_3)_4$  undergoes a structural phase transition at 360 K, a magnetic phase transition 38.5 K

(the easy-plane antiferromagnetic structure AFM2) and a spin-flip phase transition to the easy-axis antiferromagnetic structure AFM1 at 5 K. In addition, a spontaneous polarization that can be suppressed by the external magnetic field occurs in the region of existence of the AFM2 [2]. On the contrary, the  $\text{NdFe}_3(\text{BO}_3)_4$  crystal remains stable in the structure  $R32$ , undergoes a magnetic phase transition at 30.5 K (an easy-plane antiferromagnetic structure and exhibits a considerable magnetoelectric effect) [6, 7].

The  $\text{Nd}_{0.5}\text{Ho}_{0.5}\text{Fe}_3(\text{BO}_3)_4$  solid solution inherits the characteristics of both parent compounds: similar to  $\text{NdFe}_3(\text{BO}_3)_4$ ,  $\text{Nd}_{0.5}\text{Ho}_{0.5}\text{Fe}_3(\text{BO}_3)_4$  does not undergo a structural phase transition. The magnetic phase transition to the easy-plane antiferromagnetic structure occurs at 32 K and the region of existence of the easy-axis structure AFM1 expands ( $T = 9$  K). A spontaneous polarization occurs similar to  $\text{HoFe}_3(\text{BO}_3)_4$ , yet in contrast to  $\text{HoFe}_3(\text{BO}_3)_4$ , the external magnetic field suppresses the polarization only if the field is applied along the  $c$  axis, whereas a considerable magnetoelectric effect takes place in the magnetic field applied along the  $a$  axis [8].

In our previous work [9], we discovered the emergence of new lines in the Raman spectra of  $\text{Nd}_{0.22}\text{Ho}_{0.78}\text{Fe}_3(\text{BO}_3)_4$  in the region of 630  $\text{cm}^{-1}$  below the temperature of the magnetic phase transition, which was unseen in  $\text{NdFe}_3(\text{BO}_3)_4$  and  $\text{HoFe}_3(\text{BO}_3)_4$ . Perhaps, this is a specific feature of solid solutions.

In this work, we study the infrared spectra of the  $\text{Nd}_{0.5}\text{Ho}_{0.5}\text{Fe}_3(\text{BO}_3)_4$  rear-earth ferrobate solid solu-

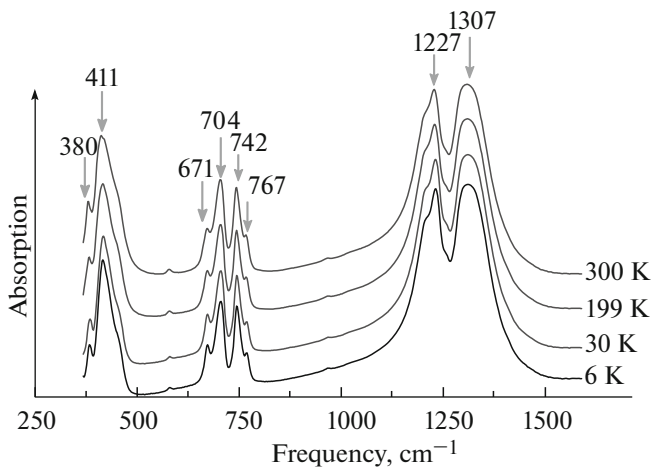


**Fig. 1.** Temperature variation of absorption spectra in the frequency range of 375–1700  $\text{cm}^{-1}$ .

tion in the spectral region of 30–1700  $\text{cm}^{-1}$  in a wide temperature range (from 6 to 300 K).

## 2. SYNTHESIS

$\text{Nd}_{0.5}\text{Ho}_{0.5}\text{Fe}_3(\text{BO}_3)_4$  single crystals were grown from melt solutions based on bismuth trimolibdate [8]. It is convenient to represent the melt-solution system as the quasi-binary form of 82 wt %  $[\text{Bi}_2\text{Mo}_3\text{O}_{12} + 3\text{B}_2\text{O}_3 + 0.25\text{Ho}_2\text{O}_3 + 0.25\text{Nd}_2\text{O}_3] + 18$  wt %  $\text{Nd}_{0.5}\text{Ho}_{0.5}\text{Fe}_3(\text{BO}_3)_4$ . The stability regions of the  $\text{Nd}_{0.5}\text{Ho}_{0.5}\text{Fe}_3(\text{BO}_3)_4$  crystals and the proportion of the components of the melt solution were determined by the direct phase probing. The saturation temperature was determined with an accuracy of  $\pm 2^\circ\text{C}$  with the use of probe crystals preliminary grown from the same melt solution on a rotating platinum rod under the conditions of spontaneous nucleation. The width  $\Delta T_{\text{met}} \approx 12^\circ\text{C}$  of the metastable phase was found as the maximum overcooling, at which nucleation had not occurred for a period of 20 h.

The melt solutions with a mass of 800 g were prepared at  $T = 1000^\circ\text{C}$  in a cylindrical platinum crucible ( $D = 100$  mm,  $H = 100$  mm) by comelting the oxides ( $\text{Bi}_2\text{O}_3$ ,  $\text{MoO}_3$ ,  $\text{B}_2\text{O}_3$ ,  $\text{Ho}_2\text{O}_3$ ,  $\text{Nd}_2\text{O}_3$ ,  $\text{Fe}_2\text{O}_3$ ) in the proportion given by the above formula. The crucible was placed to a crystallization furnace, where the temperature upward decreased from the crucible bottom with a vertical gradient of  $1\text{--}2^\circ\text{C}/\text{cm}$ . The melt solution was homogenized at  $T = 1050^\circ\text{C}$  for 24 h. To maintain homogeneity, the melt solution was stirred. The saturation temperature determined with the use of probe crystals appeared to be  $965 \pm 2^\circ\text{C}$ . First, the crystal with a size of  $\sim 1$  mm were grown in the regime of spontaneous nucleation at the temperature  $T = T_{\text{sat}} - (15\text{--}20)^\circ\text{C}$ . The crystal holder with the grown small crystals was taken away without changing the

furnace temperature. These crystals were then used as nuclei.

Next, ten visually quality nuclei were fixed to a circular platinum crystal holder. The holder was immersed into the melt solution at the temperature  $T = T_{\text{sat}} + 7^\circ\text{C}$  and reversible rotation at the angular velocity  $\omega = 30$  rpm and a period of 1 min was switched on. After 15 min, the temperature was decreased to  $T = T_{\text{sat}} - 7^\circ\text{C}$ . Then the temperature of the melt solution was decreased at an increasing rate of  $1\text{--}3^\circ\text{C}$  per day so that the growth rate of the crystals were no higher than 0.5 mm per day. After completion of the growth, the rod was elevated above the surface of the melt solution and cooled to room temperature with the furnace power switched off. As a result, crystals with a size of 5–7 mm were grown.

## 3. RESULTS AND DISCUSSION

The experimental investigation of the IR spectra of  $\text{Nd}_{0.5}\text{Ho}_{0.5}\text{Fe}_3(\text{BO}_3)_4$  was carried out on a Bruker VERTEX 80V vacuum Fourier spectrometer in the spectral range of 30 to 1700  $\text{cm}^{-1}$  with a spectral resolution of  $0.2$   $\text{cm}^{-1}$ . The measurements were carried out with an Optistat TM AC-V 12a 0.25W@4K cryostat in the temperature range of 6 to 300 K. In our previous work, we studied a  $\text{HoFe}_3(\text{BO}_3)_4$  crystal by the same technique; a more detailed description of the experiment can be found in [10].

The structure of  $\text{ReFe}_3(\text{BO}_3)_4$  rear-earth ferroborate crystals with the symmetry of space group  $R32$  was repeatedly described and analyzed in earlier works [2, 6]; the comprehensive group-theory analysis of the vibrational spectrum was also carried out [10]. The basic structural elements of rear-earth ferrobates are triangles (there are four  $\text{BO}_3$  molecular groups per unit cell, one with the symmetry  $D_3$  and three with the symmetry  $C_2$ ),  $\text{FeO}_6$  octahedra, and  $\text{ReO}_6$  triangular prisms that are largely localized. Accordingly, the vibrational spectrum of rare-earth ferrobates is formed by internal vibrations of  $\text{BO}_3$ ,  $\text{FeO}_6$  and  $\text{ReO}_6$  groups. A complete correlation scheme of the vibrational modes of  $\text{ReFe}_3(\text{BO}_3)_4$  of space group  $R32$  for the  $\text{BO}_3$  molecular group and  $\text{Re}$  and  $\text{Fe}$  ions was presented in [11].

Figure 1 shows the evolution of the absorption spectra in the range of 375–1700  $\text{cm}^{-1}$ . As is seen in Fig. 1, the spectra does not exhibit noticeable changes with a decrease in temperature. According to the correlation diagram of internal vibrations (Fig. 2), the two most intense broad bands with maxima at 1227 and 1307  $\text{cm}^{-1}$  are caused by the valence oscillations  $\nu_3$  of  $\text{BO}_3^{3-}$  complexes with the local symmetries  $D_3$  and  $C_2$ , respectively. The band at 1227  $\text{cm}^{-1}$  has a complicated structure, which is associated with lifted degeneracy of this mode in a low-symmetry environment ( $C_2$ ).

Ion	Vibration type [12]	Frequency [12], $\text{cm}^{-1}$	Free ion symmetry	Site symmetry	Crystal symmetry
B(1)O <sub>3</sub>			$D_{3h}$	$D_3$	$D_3$
	$\nu_1$	939–1060	$A'_1$	$A_1$	$A_1$
	$\nu_2$	650–740	$A''_2$	$A_2$	$A_2$
	$\nu_3$	1330–1490	$E'$	$E$	$E$
B(2)O <sub>3</sub>			$D_{3h}$	$C_2$	$D_3$
	$\nu_1$	939–1060	$A'_1$	$A$	$A_1$ $E$
	$\nu_2$	650–740	$A''_2$	$B$	$A_2$ $E$
	$\nu_4$	1330–1490	$E'$	$A$ $B$	$A_1$ $E$ $A_2$ $E$
	$\nu_3$	545–606	$E'$	$A$ $B$	$A_1$ $E$ $A_2$ $E$

Fig. 2. Correlation diagram of internal oscillations of the  $\text{BO}_3$  molecular groups in the  $\text{Nd}_{0.5}\text{Ho}_{0.5}\text{Fe}_3(\text{BO}_3)_4$  crystal.

A low-intensity line at  $900\text{ cm}^{-1}$  also belongs to oscillations of the  $\text{BO}_3$  molecular group with the symmetry  $C_2$ . The full-symmetry vibration  $\nu_1$  occurring in

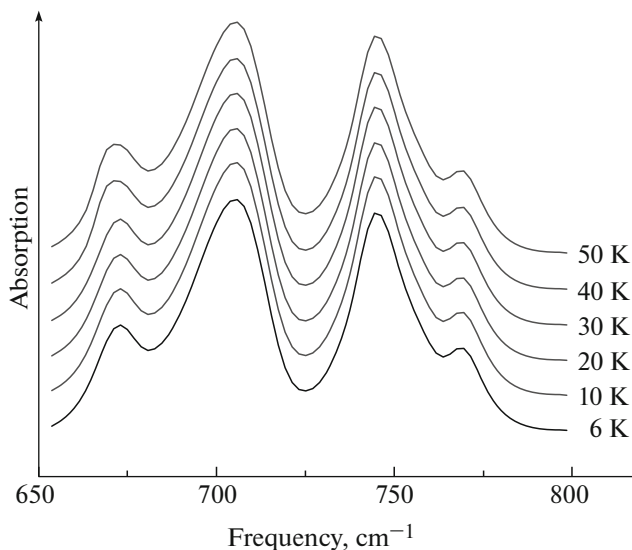


Fig. 3. Spectral region of  $650\text{--}800\text{ cm}^{-1}$ .

this frequency region (Fig. 2) is inactive in the IR spectrum of a free  $\text{BO}_3$  ion and its activation in the crystal can be caused by a distortion of the ion structure in the crystal environment or by coupling of the modes (Davydov splitting). A low intensity of this line indicates a low magnitude of the above distortions.

The spectral region of  $650\text{--}800\text{ cm}^{-1}$  corresponds to the deformation vibrations  $\nu_4$  and  $\nu_2$  of a free  $\text{BO}_3$  group. According to [12], planar molecular groups  $XY_3$  should obey the condition  $\nu_4 < \nu_2$ . Seemingly, the groups of lines at  $670\text{--}704$  and  $742\text{--}767\text{ cm}^{-1}$  correspond to the vibrations  $\nu_4$  and  $\nu_2$ , respectively (Fig. 3).

The Raman spectra of the mixed  $\text{Nd}_{0.22}\text{Ho}_{0.78}\text{Fe}_3(\text{BO}_3)_4$  crystal exhibit the emergence of new lines near  $630\text{ cm}^{-1}$  below the magnetic phase transition temperature. We thoroughly studied the evolution of the spectra of  $\text{Nd}_{0.5}\text{Ho}_{0.5}\text{Fe}_3(\text{BO}_3)_4$  with temperature but did not observe any noticeable changes below the magnetic phase transition (Fig. 3). This implies that the lines activated by the magnetic phase transition are inactive in the IR spectrum, i.e., nonpolar.

Figure 4 shows the IR spectrum of  $\text{Nd}_{0.5}\text{Ho}_{0.5}\text{Fe}_3(\text{BO}_3)_4$  in the range from  $100$  to  $600\text{ cm}^{-1}$

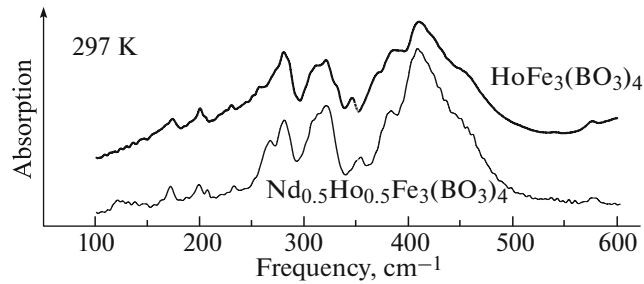


**Fig. 4** Comparison of the absorption spectra of  $\text{HoFe}_3(\text{BO}_3)_4$  and  $\text{Nd}_{0.5}\text{Ho}_{0.5}\text{Fe}_3(\text{BO}_3)_4$  crystals in the frequency range of  $100\text{--}600\text{ cm}^{-1}$ .

in comparison with the IR spectrum of  $\text{HoFe}_3(\text{BO}_3)_4$ . Clearly, the contour is quite complicated in this spectrum range and consists of a large number of peaks. This frequency range corresponds to internal vibrations of  $\text{FeO}_6$  octahedra and  $\text{ReO}_6$  triangular prisms and to external vibrations. Intense lines near  $450$  and  $280\text{ cm}^{-1}$  seemingly correspond to internal vibrations of the  $\text{FeO}_6$  octahedron [13]. Doping by neodymium did not lead to considerable changes in this spectrum range, despite the fact that  $\text{HoFe}_3(\text{BO}_3)_4$  appears in the phase  $P3_121$  at room temperature, whereas  $\text{Nd}_{0.5}\text{Ho}_{0.5}\text{Fe}_3(\text{BO}_3)_4$  is in the phase with the symmetry  $R32$ . Such a small difference can be caused by several reasons.

First, the IR spectrum of  $\text{HoFe}_3(\text{BO}_3)_4$  exhibits insignificant changes at the structural phase transition. Despite tripling of the unit cell, owing to considerable localization of the internal modes of  $\text{BO}_3$ ,  $\text{FeO}_6$  and  $\text{ReO}_6$  complexes, the line splitting can be seen only in the Raman spectra, where the lines of scattered light are narrower.

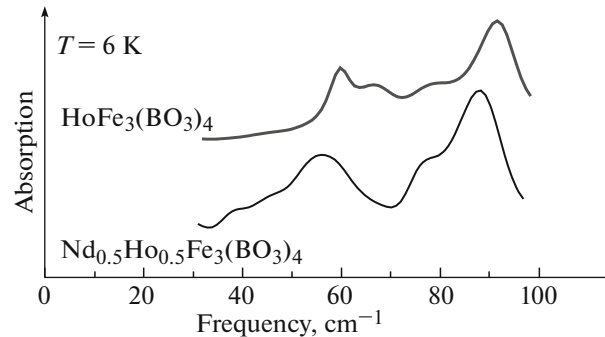
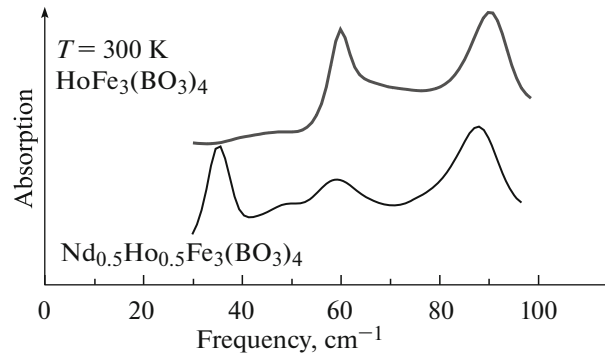


**Fig. 5.** Comparison of the absorption spectra of  $\text{HoFe}_3(\text{BO}_3)_4$  and  $\text{Nd}_{0.5}\text{Ho}_{0.5}\text{Fe}_3(\text{BO}_3)_4$  crystals in the frequency range of  $30\text{--}100\text{ cm}^{-1}$  at temperatures of  $300$  and  $6\text{ K}$ .

Second, the composition under investigation is a solid solution, in which Nd and Ho are randomly distributed over the  $3a$  positions in the crystal. The difference between the ionic radii of Ho and Nd is quite noticeable,  $0.89$  and  $0.98\text{ \AA}$ , respectively. As a consequence, local distortions appear in the structure, which may affect the vibration frequencies of molecular groups. However, one can hardly expect that these distortions are considerable, since both the experi-

Calculated infrared-active vibration frequencies of  $\text{HoFe}_3(\text{BO}_3)_4$  and  $\text{NdFe}_3(\text{BO}_3)_4$  crystals ( $\text{cm}^{-1}$ )

Symmetry type $A_2$		Symmetry type $A_2$		Symmetry type $E$		Symmetry type $E$	
$\text{NdFe}(\text{BO}_3)_4$	$\text{HoFe}_3(\text{BO}_3)_4$	$\text{NdFe}(\text{BO}_3)_4$	$\text{HoFe}_3(\text{BO}_3)_4$	$\text{NdFe}_3(\text{BO}_3)_4$	$\text{HoFe}_3(\text{BO}_3)_4$	$\text{NdFe}_3(\text{BO}_3)_4$	$\text{HoFe}_3(\text{BO}_3)_4$
97	96	734	748	113	109	561	567
158	161	1284	1287	156	160	641	646
188	193			203	210	660	669
207	212			218	222	691	702
243	248			249	250	716	726
257	262			267	269	963	960
282	287			296	300	1232	1237
309	313			341	346	1252	1261
636	642			358	366	1285	1288
718	728			445	448		

mental data [11] and the results of our calculations indicate that the vibration frequencies of  $\text{HoFe}_3(\text{BO}_3)_4$  are very close (see the table). The calculation was performed with the use of the LADY software package [14]. Simulation of the lattice dynamics taking into account the probability of occupation by neodymium and holmium atoms was carried out in the modified random-substitution model [15].

Considerable changes can be expected at ultimately low frequencies corresponding to the oscillations of the rare-earth Ho and Nd ions. Indeed, the mixed crystal exhibits two additional peaks below  $100\text{ cm}^{-1}$  at frequencies of  $35$  and  $48\text{ cm}^{-1}$ , which presumably correspond to oscillations of neodymium atoms (Fig. 5). As is seen from comparison of the low-frequency spectra of  $\text{Nd}_{0.5}\text{Ho}_{0.5}\text{Fe}_3(\text{BO}_3)_4$  and  $\text{HoFe}_3(\text{BO}_3)_4$ , the lines near  $60$  and  $90\text{ cm}^{-1}$  appear for both compounds, are very weakly shifted under doping by neodymium and correspond to oscillations of Ho ions.

### CONCLUSIONS

Investigation of the infrared spectra of  $\text{Nd}_{0.5}\text{Ho}_{0.5}\text{Fe}_3(\text{BO}_3)_4$  in the frequency range of  $30$ – $1700\text{ cm}^{-1}$  at temperatures from  $6$  to  $300\text{ K}$  has shown that changes associated with structural phase transitions do not occur. Neither the IR spectra of  $\text{Nd}_{0.5}\text{Ho}_{0.5}\text{Fe}_3(\text{BO}_3)_4$  are affected by the magnetic transition. Insignificant difference between the IR spectra of  $\text{Nd}_{0.5}\text{Ho}_{0.5}\text{Fe}_3(\text{BO}_3)_4$  and  $\text{HoFe}_3(\text{BO}_3)_4$  indicate that the IR spectra of rare-earth ferrobates are largely formed by internal vibrations of the  $\text{BO}_3$ ,  $\text{FeO}_6$ , and  $\text{ReO}_6$  groups, which are almost immune to structural changes and replacement of the rare-earth cation, as confirmed by semiempirical calculations of the lattice dynamics. Changes are seen only in the low-frequency region of the spectrum, where the new lines associated with the oscillations of Nd appear.

### ACKNOWLEDGMENTS

This study was supported in part by the Russian Foundation for Basic Research (project no. 12-02-00825).

### REFERENCES

1. A. A. Mukhin, G. P. Vorob'ev, V. Yu. Ivanov, A. M. Kadomtseva, A. S. Narizhnaya, A. M. Kuz'menko, Yu. F. Popov, L. N. Bezmaternykh, and I. A. Gudim, *JETP Lett.* **93** (5), 275 (2011).
2. C. Ritter, A. Vorotynov, A. Pankrats, G. Petrakovskii, V. Temerov, I. Gudim, and R. Szymczak, *J. Phys.: Condens. Matter* **20**, 365209 (2008).
3. A. A. Demidov and D. V. Volkov, *Phys. Solid State* **53** (5), 985 (2011).
4. I. A. Gudim, E. V. Eremin, and V. L. Temerov, *J. Cryst. Growth* **312**, 2427 (2010).
5. A. M. Kadomtseva, Yu. F. Popov, G. P. Vorob'ev, A. P. Pyatkov, S. S. Krotov, K. I. Kamilov V. Yu. Ivanov, A. A. Mukhin, A. K. Zvezdin, A. M. Kuz'menko, L. N. Bezmaternykh, I. A. Gudim, and V. L. Temerov, *Low Temp. Phys.* **36** (6), 511 (2010).
6. M. N. Popova, E. P. Chukalina, T. N. Stanislavchuk, B. Z. Malkin, A. R. Zakirov, E. Antic-Fidancev, E. A. Popova, L. N. Bezmaternykh, and V. L. Temerov, *Phys. Rev. B: Condens. Matter* **75**, 224435 (2007).
7. M. Janoschek, P. Fischer, J. Schefer, B. Roessli, V. Pomjakushin, M. Meven, V. Petricek, G. Petrakovskii, and L. Bezmaternykh, *Phys. Rev. B: Condens. Matter* **81**, 094429 (2010).
8. R. P. Chaudhury, F. Yen, B. Lorenz, Y. Y. Sun, L. N. Bezmaternykh, V. L. Temerov, and C. W. Chu, *Phys. Rev. B: Condens. Matter* **80**, 104424 (2009).
9. A. S. Krylov, S. N. Sofronova, I. A. Gudim, and A. N. Vtyurin, *Solid State Commun.* **174**, 26 (2013).
10. S. N. Sofronova, Yu. V. Gerasimova, A. N. Vtyurin, I. A. Gudim, N. P. Shestakov, and A. A. Ivanenko, *Vib. Spectrosc.* **72**, 20 (2014).
11. D. Fausti, A. A. Nugroho, P. H. M. van Loosdrecht, S. A. Klimin, M. N. Popova, and L. N. Bezmaternykh, *Phys. Rev. B: Condens. Matter* **74**, 024403 (2006).
12. K. Nakamoto, *Infrared and Raman Spectra of Inorganic and Coordination Compounds* (Wiley, New York, 1986; Mir, Moscow, 1991).
13. M. I. Pashchenko, V. A. Bedarev, V. I. Kut'ko, L. N. Bezmaternykh, and V. L. Temerov, *Low Temp. Phys.* **36** (7), 638 (2010).
14. M. B. Smirnov and V. Yu. Kazimirov, *LADY: Software for Lattice Dynamics Simulations* (JINR Communications, Dubna, 2001), E14-2001-159.
15. I. F. Chang and S. S. Mitra, *Phys. Rev.* **172**, 924 (1986).

*Translated by A. Safonov*